Monitoring fin and blue whales in the Lower St. Lawrence Seaway with onshore seismometers

Alexandre P. Plourde[1,2] and Mladen R. Nedimović[2]

[1] Geological Survey of Canada (Atlantic). 1 Challenger Dr., Dartmouth, Nova Scotia, Canada, B2Y 4A2.
[2] Dalhousie University. 1355 Oxford St., Halifax, Nova Scotia, Canada, B3H 3Z1.

Corresponding Author: A. P. Plourde, ap.plourde@dal.ca.

Abstract

The Lower St. Lawrence Seaway (LSLS), in eastern Canada, is an important habitat for several species of endangered baleen whale. As we seek to reduce the hazards that these endangered species face from human activity, there is increasing demand for detailed knowledge of their habitat use. Only a sparse network of hydrophones exists in the LSLS to remotely observe whales. However, there is also a network of onshore seismometers, designed to monitor earthquakes, that have sufficiently high sample rates to record fin and blue whale calls. We present a simple method for detecting band-limited, regularly repeating calls, such as the 20 Hz calls of fin and blue whales, and apply the method to build a catalog of fin and blue whale detections at 14 onshore seismometers across the LSLS, over approximately a four-year period. The resulting catalog contains >600000 fin whale calls and >60000 blue whale calls. Individual calls are rarely detected at more than one seismometer. Fin whale calls recorded onshore appear to travel mainly through solid earth, rather than only entering the earth at the shoreline, and they often have a complex ∼2 s sequence of P-like and S-like phases. Onshore seismometers provide a valuable, previously unused source of data for monitoring baleen whales. However, in the LSLS, the current seismometer network cannot provide high-precision whale tracking alone, so a denser deployment of onshore and/or offshore seismometers is required.

Keywords

Baleen whale, acoustic monitoring, seismology, marine-mammal tracking, conservation, mitigation

1 Introduction

Baleen whales face a variety of hazards from human activity including vessel strikes, entanglement in fishing gear, and noise pollution (Pettis et al., 2021; Ramp et al., 2014, 2021; Rolland et al., 2012). Demand for knowledge of baleen whale habitat use and migration behavior is increasing as governments attempt to mitigate these hazards. In the Lower St. Lawrence Seaway (LSLS), a major shipping corridor in eastern Canada, conservation efforts are largely focused on the critically-endangered North Atlantic Right Whale (NARW, *E.glacialis*), although fin whales (*B. physalus*) and blue whales (*B. musculus*) are also present in the LSLS and have elevated conservation status.

Acoustic monitoring is the primary way of remotely observing whales. Whereas NARW vocalizations, or calls, are mainly in the 50–350 Hz range (e.g. Parks et al., 2009), fin and blue whales both have common "20 Hz" calls, that are their primary signal used for monitoring. In the case of fin whales, the calls consist of a 1 s pulse in the ∼18–23 Hz band, repeating every ∼12 s (Watkins et al., 1987). Blue whales have at least two common infrasonic (∼18 Hz) calls, including 8 s tonal "A" notes and 10 s downsweep "B" notes, which often appear together, separated by ∼5 s in "AB" calls that repeat every 73 s (Mellinger and Clark, 2003).

To acoustically monitor whales, Fisheries and Oceans Canada relies on a sparse network of hydrophones (Roy et al., 2018; Simard et al., 2019; Kirsebom et al., 2020), that does not allow localization of calls. However, the 20 Hz calls are sufficiently low-frequency that they are often recorded on ocean-bottom seismometers (OBS) designed for earthquake monitoring (Gaspà Rebull et al., 2006; Dunn and Hernandez, 2009; Wilcock, 2012; Harris et al., 2018), and Kuna and Nábělek (2021) have demonstrated that the fin whale calls penetrate several kilometers into the Earth's crust. There are no ocean-bottom seismometers in the LSLS, but there is a network of land seismometers along LSLS shorelines (Fig. 1) operated by Earthquakes Canada (2021) for earthquake monitoring (e.g. Plourde and Nedimović, 2021).

This study explores the potential use of onshore seismometers to monitor fin and blue whales in the LSLS using data from 14 stations (Fig. 1), from October 2015 to February 2020. To the best of our knowledge, this is the first attempt to use land seismometers to monitor marine life. Each seismometer records at 100 sps, although several were upgraded from lower sampling rates during this timespan. We first outline a

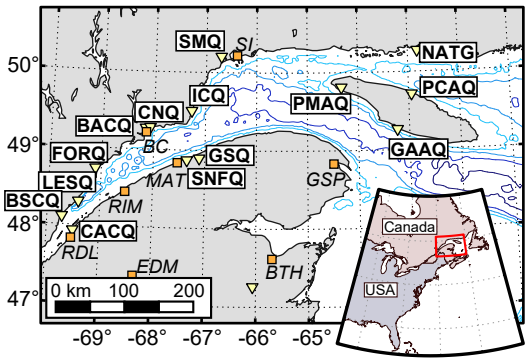

Figure 1. Map of the LSLS. Seismometers used in this study are labeled with yellow triangles and their 3–4 letter station name. Bathymetry is contoured at intervals of 100 m; the deepest contours (darkest blue) being at 400 m depth. Cities and towns are labeled with orange rectangles and short-forms in italics: BC = Baie-Comeau, BTH = Bathurst, EDM = Edmunston, GSP = Gaspé, MAT = Matane, RDL = Rivière-du-Loup, RIM = Rimouski, SI = Sept-Îles. The inset map (lower right) shows the position of the larger map with respect to eastern North America.

simple method for detecting fin and blue whale 20 Hz calls (or other band-limited, regularly repeating calls), then present our resulting catalogs of detections.

2 Methods

Fin and blue whale calls have been detected with a wide variety of algorithms, many of which are described in a review by Mellinger et al. (2007). Some of the more widely used methods, including those used in the LSLS (Mouy et al., 2009; Roy et al., 2018), involve template-matching or machine-learning, and therefore require an existing collection of manually confirmed detections. Because we did not know how signals from fin and blue whale calls are distorted during transmission through shallow earth structures, or how that distortion varies from one seismometers to another, we chose to design a method that does not require input templates. Our new method instead relies on characteristic recurrence intervals of the two respective 20 Hz calls, specifically ∼12 s for fin whales and ∼73 s for blue whales.

Here we outline our method for detecting fin whale calls at a seismometer:

1. Zero-phase bandpass filter one day of data to 12–32 Hz. Note that the data usually consists of three orthogonal geophones (two horizontal, one vertical) as shown in Fig. 2a, but in some cases there is only a single (vertical) component.

2. Compute power spectrogram $A(t, f)$. For each component, compute a power spectrogram with 1 s

windows, 0.5 s overlap, for 48 logarithmically-spaced frequency bins spanning 12–32 Hz. Sum across components and smooth with a 3×3 Gaussian filter (Fig. 2b).

3. Compute the fin whale call index (e.g. Širović et al., 2015; Pilkington et al., 2018):

$$R(t) = \frac{\int_{18Hz}^{21Hz} A(t,f)df}{\int_{12Hz}^{17Hz} A(t,f)df + \int_{23Hz}^{32Hz} A(t,f)df}. \quad (1)$$

Zero-phase bandpass filter $R(t)$ to 0.029–0.15 Hz, or equivalently 35 s to 7 s periods (Fig. 2c).

4. Compute a secondary power spectrogram $P(t,T)$, from $R(t)$, using 120 s windows with no overlap. Use 200 logarithmically-spaced periods spanning 7–35 s (Fig. 2d). Note that we refer to period (T) instead of frequency here simply for the convenience of integer values.

5. For each 120 s window, compute the ratio $W(t)$ as the sum of energy near the characteristic 12 s period over the sum of energy at adjacent periods, specifically :

$$W(t) = \frac{\int_{10.0s}^{13.8s} P(t,T)dT}{\int_{14.5s}^{35s} P(t,T)dT + \int_{7.0s}^{9.5s} P(t,T)dT}. \quad (2)$$

A detection is triggered when $W(t)$ exceeds an empirically chosen threshold $W_{\min} = 3.0$.

6. Categorize days as "active" if there are five or more detections (i.e. at least 10 minutes with calls) or "quiet" otherwise. We assume detections on quiet days to be false.

7. For each detection, compute the number and time of individual calls by recursively selecting the maximum value of $R(t)$ in the 120 s window that is not within 9.5 s of a previous selection or lower than twice the median value of $R(t)$. Estimate the signal-to-noise ratio (SNR) from the 18–21 Hz seismogram as $\mathrm{SNR} = 10\log_{10}(\frac{P_1}{P_0})$, where P_1 is the mean-square value of a 1 s window centered on the maximum $R(t)$ value and P_0 is the mean-square value of the window 3.8 s to 0.8 s before that center-time. For three-component geophones, P_1 and P_0 are summed across waveform components.

The $W = 3.0$ threshold approximately maximizes the ratio $\frac{\sigma_d}{\mu_d}$, where σ_d and μ_d are the standard deviation and mean detections per day, respectively (note that these values are computed prior to culling detections

from days with fewer than five total detections). This selection is based on an assumption that i) fin whales travel slowly, i.e. they commonly stay in the detection radius of a given seismometer for a substantial portion of the day, and ii) their "songs" generally last for much more than 10 minutes per day. Depending on the periodicity of $R(t)$ to trigger detections assumes that the signal is not completely saturated with fin whale calls, as has been observed to occur sometimes on hydrophone data (e.g. Pilkington et al., 2018).

We detect blue whale calls with an almost identical method, except with the following changes to each step:

1. The waveform bandpass extends to lower frequencies, 10–32 Hz.

2. Spectrograms are computed with 2 s sample intervals, 1 s overlap.

3. The blue whale call index is computed as:

$$R(t) = \frac{\int_{16.0Hz}^{18.5Hz} A(t,f)df}{\int_{10Hz}^{14Hz} A(t,f)df + \int_{21Hz}^{32Hz} A(t,f)df}, \tag{3}$$

   and then bandpass filtered from 180 s to 40 s periods.

4. The power spectrogram $P(t,T)$ is computed for 720 s windows, with periods spanning 40 to 180 s.

5. The ratio $W(t)$ targets the 73 s recurrence period and is computed as:

$$W(t) = \frac{\int_{66s}^{76s} P(t,T)dT}{\int_{80s}^{180s} P(t,T)dT + \int_{40s}^{62s} P(t,T)dT}. \tag{4}$$

   We select a detection threshold $W_{\min} = 1.5$ in the same empirical manner as was used for fin whales.

6. Only three detections (36 minutes) are required for a day to be considered active.

7. When counting individual calls, the minimum time between calls is 65 s, P_1 is measured over a 4 s window centered on the maximum $R(t)$, and the window for P_0 extends 20 s to 5 s before that center-time. SNR is computed on a 16–18.5 Hz seismograms.

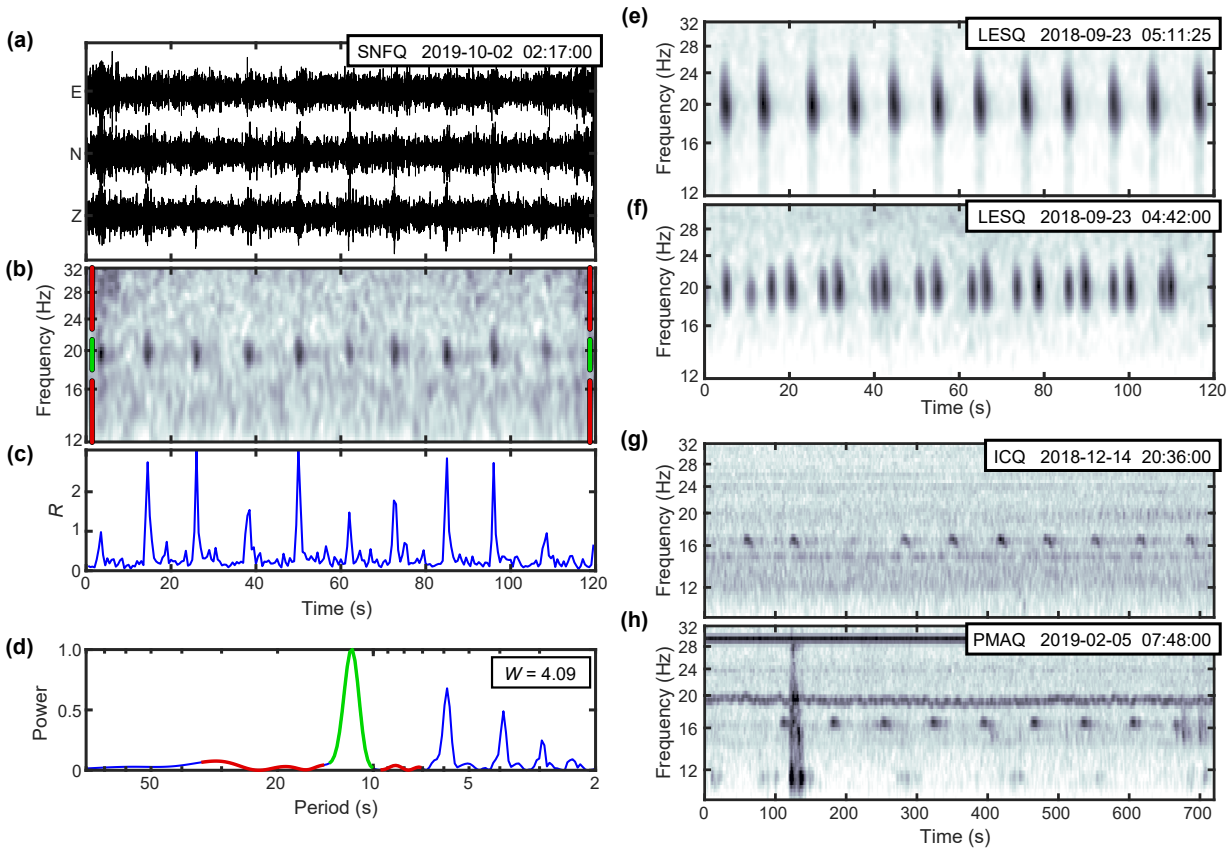

Figure 2. Examples of fin and blue whale detections. (a)-(d) illustrate the detection process for a fairly typical fin whale recording at SNFQ. (a) 120 s long three-component seismogram bandpassed at 12–32 Hz. (b) 12–32 Hz spectrogram of the seismograms summed across components and smoothed. Green and red lines show the bands used in the numerator and denominator, respectively, of the fin whale call index R. (c) R computed from the spectrogram. (d) Periodogram of R. Green and red lines show the bands used in the numerator and denominator, respectively, of the fin whale power ratio W. (e) Fin whale detection spectrogram from LESQ whose fourth call has the highest SNR in the dataset (44 dB). (f) Another fin whale spectrogram at LESQ that appears to show two whales singing simultaneously. (g) Example of a blue whale detection spectrogram at station ICQ. (h) Blue whale detection at PMAQ with $W = 22.8$, the highest among all blue whale detections, despite noisy bands at ∼19 Hz and ∼30 Hz, and a high-noise event at $t = 130$ s. Note that all times shown are in UTC.

3 Results

The number of fin and blue whale detections per day are illustrated in Figs 3 and 4, respectively. Table 1 displays the number of fin-whale active days (D_A) and quiet days (D_Q) for each seismometer, along with corresponding number of detections (N_A, N_Q), number of individual calls (C_A, C_Q), and the median SNR (SNR_A, SNR_Q) of those calls. Table 2 displays the corresponding data for blue whales.

Station LESQ, near the mouth of the Saguenay River, records by far the most fin whale activity, with the highest D_A, N_A, and C_A of any station. Its detections also have the highest median SNR (16.2 dB, Table 1), and include one call of SNR = 44 dB, the highest SNR recorded in this study. A spectrogram including that call is shown in Fig. 2e; note that at such high SNR energy is visible throughout the entire 12–32 Hz range of the spectrogram. Fig. 2f shows another detection at LESQ, an example of what appears to be two fin whales singing simultaneously. In total, the dataset contains 61884 fin whale detections (including only those on active days), consisting of 617251 calls. Similar to Roy et al. (2018), we find that fin whale calls are predominantly heard in autumn and early winter; 97% of detections occur in the September–January period.

The number of blue whale detections is far smaller than that for fin whales, with totals of 6963 detections and 60155 calls (active days only), but the two catalogs have some similar trends. Blue whale detections also occur mainly in the autumn and early winter, with 91% of detections occurring from September–January. Their detection locations are skewed, relatively compared to fin whales, to the east. Stations near the open Gulf of St. Lawrence such as ICQ, SMQ, and PMAQ have rich catalogs whereas the furthest upriver stations, BSCQ and CACQ, have 0 and 4 detections, respectively. ICQ has the maximum D_A, N_A, and C_A, but as was the case for fin whales, LESQ has the highest median SNR at 9.1 dB.

It was extremely rare for detections of either species to occur at multiple stations at the same time. Even at stations BACQ and CNQ, which are only 7 km apart, there was only 7% overlap in detection times (for both fin and blue whales). Most pairs of neighboring stations are much farther apart (10s of km) and have ∼1% overlap.

We estimate false detection rates for each species as $\sum N_Q / \sum D_Q$ (summing over the 14 stations), which returns 0.6 and 0.15 detections per seismometer, per day for fin and blue whales, respectively. These are

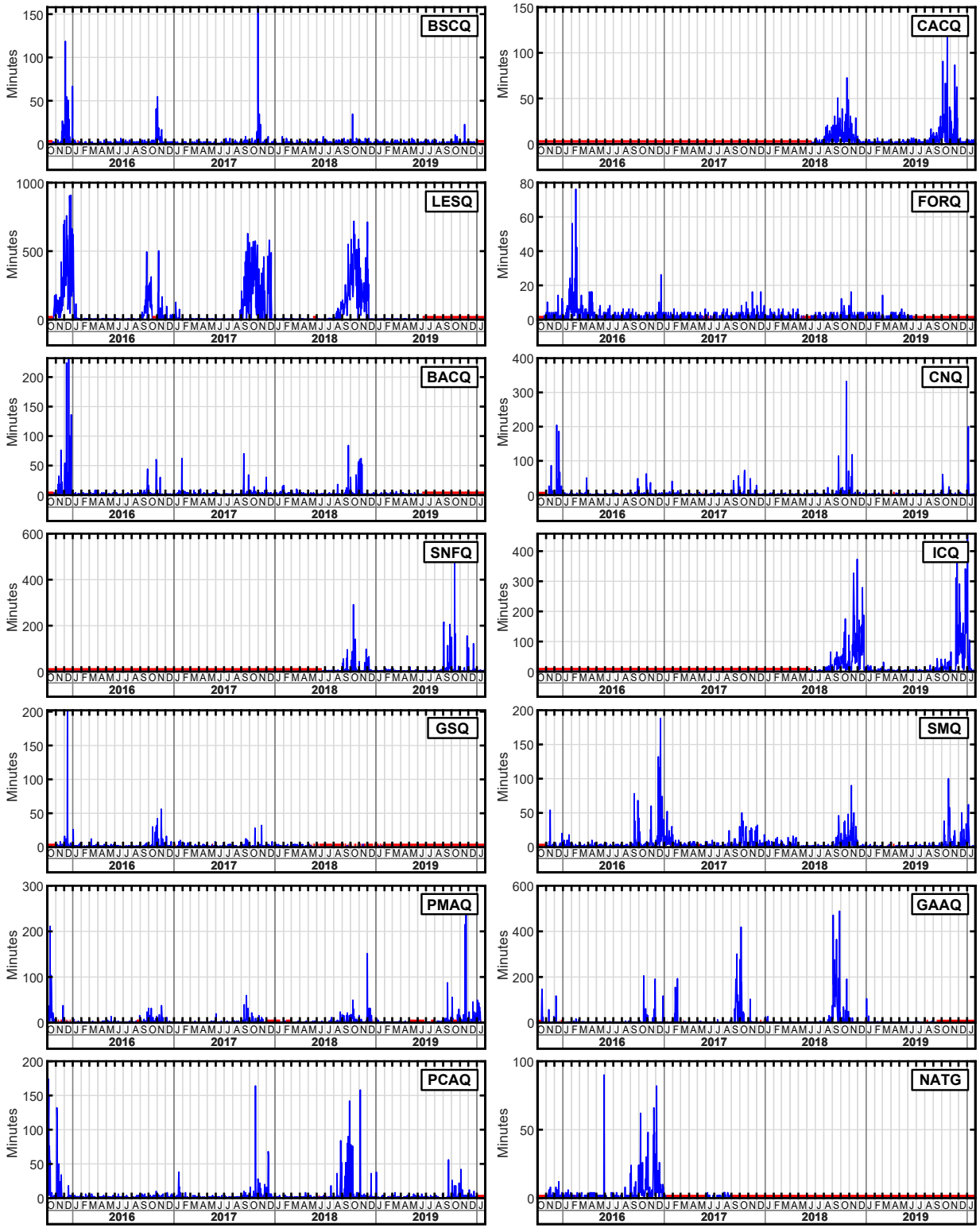

Figure 3. Minutes of fin whale detections per day at the 14 seismometers shown in Figure 1. Red lines indicate periods when the seismometer was not operating.

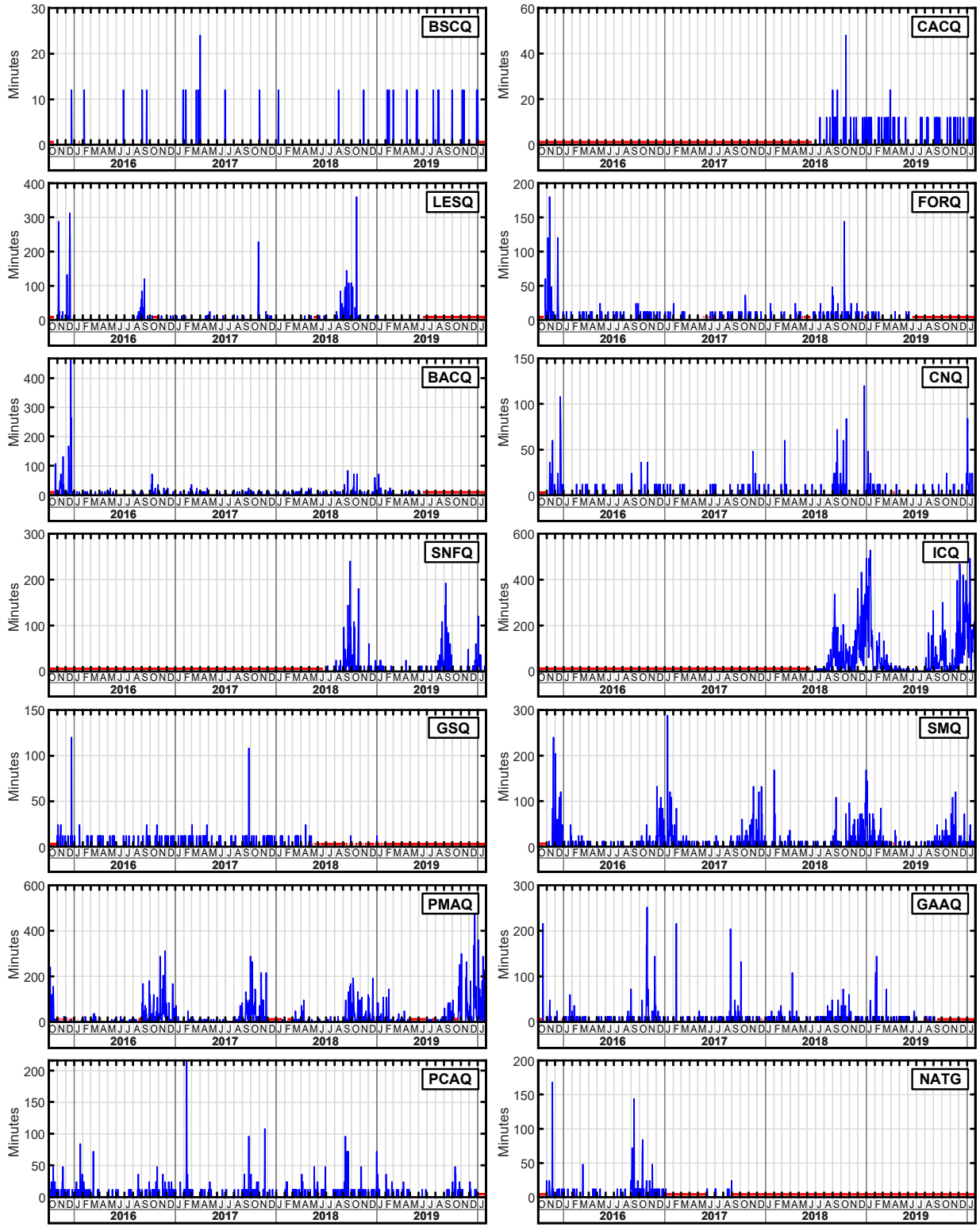

Figure 4. Minutes of blue whale detections per day at the 14 seismometers shown in Figure 1. Red lines indicate periods when the seismometer was not operating.

Table 1. Fin whale detection statistics by station, separated into those on active days and quiet days. Columns indicate the total number of days, total number of detections (120 s windows), total number of calls, and the median SNR of those calls. Stations are ordered west to east.

	Active days (≥ 5 detections)				Quiet days (< 5 detections)			
	Days (D_A)	Det. (N_A)	Calls (C_A)	SNR_A	Days (D_Q)	Det. (N_Q)	Calls (C_Q)	SNR_Q
BSCQ	35	572	5597	8.71	1461	566	4306	2.24
CACQ	85	1096	10231	5.55	516	412	3328	3.36
LESQ	336	37432	386999	16.16	956	458	3864	3.34
FORQ	37	349	3212	1.78	1213	789	6913	2.6
BACQ	45	1030	9192	4.2	1287	737	5631	2.51
CNQ	66	1458	14412	6.32	1468	1040	9560	3.22
SNFQ	51	1892	18358	7.72	548	374	2655	2.57
ICQ	198	6987	63859	5.39	407	413	3125	2.52
GSQ	24	350	3469	7.6	928	418	3793	3.27
SMQ	162	2241	21802	5.79	1377	1065	9779	3.34
PMAQ	108	1638	14837	5.29	1273	783	6450	3.11
GAAQ	110	4813	46877	7.61	1257	713	6231	3.15
PCAQ	64	1508	14001	6.02	1452	757	6566	3.26
NATG	37	518	4405	3.13	488	299	2343	2.78

only rough estimates, as there are of course some false detections on active days, and there will occasionally be isolated true detections on quiet days. We suggest these false detection rates are satisfactorily low, such that exceeding the active-day threshold with only false detections should be extremely rare events. This is least valid for blue whale detections—for which we only require three detections for a station to be considered active—at stations like SMQ and PMAQ with relatively high false detection rates. In both of those cases, if we randomly distribute their N_Q detections over D_Q days in a Monte Carlo simulation, we find that is reasonable to expect that $\sim$3 days are falsely considered active, which is still a small proportion of the 107 and 199 active days at SMQ and PMAQ.

Fig. 5 examines the waveforms of five fin whale calls, including high-SNR calls at LESQ shown in Fig. 2e,f. Fig. 5a,b shows the maximum SNR call, whose waveforms appear as a $\sim$1 s pulse, consistent with the standard duration of fin whale calls. There does appear to be a second phase arriving approximately 0.4 s after the onset of the call, visible mainly on the north component. The E–N and E–Z planes of Fig. 5b could be interpreted to suggest that the call is a P-wave arriving from the east. However, despite having an even more compact pulse, the second call shown (Fig. 5c,d) has highly elliptical motions, and the long axes of the three ellipses (in the E–N, E–Z, and N–Z planes) are inconsistent with a simple P-wave arrival. The final three calls shown (Fig. 5e–j) have much more complex waveforms, each with at least two distinct phases. Perhaps most notable is the arrival at ICQ (Fig. 5g,h) that has an initial P-like pulse with strong

Table 2. Blue whale detections by station. See Table 1 caption for details

	Active days ($\geq$ 3 detections)				Quiet days ($<$ 3 detections)			
	Days (D_A)	Det. (N_A)	Calls (C_A)	SNR$_A$	Days (D_Q)	Det. (N_Q)	Calls (C_Q)	SNR$_Q$
BSCQ	0	0	0	–	1496	30	228	2.14
CACQ	1	4	30	2.23	600	65	471	1.89
LESQ	30	318	2983	9.08	1262	76	654	4.93
FORQ	16	104	891	2.87	1234	127	1017	1.72
BACQ	26	202	1718	3.27	1306	186	1404	1.48
CNQ	19	98	923	5.25	1515	117	1025	2.76
SNFQ	40	251	2210	4.84	559	101	788	2.23
ICQ	255	3172	26572	2.97	350	152	1118	1.78
GSQ	3	22	198	4.29	949	119	1023	2.6
SMQ	107	660	6028	3.52	1432	380	3314	2.43
PMAQ	199	1665	14437	3.49	1182	309	2524	2.69
GAAQ	39	268	2485	6.24	1328	235	1979	2.53
PCAQ	27	136	1163	2.7	1489	240	1990	2.2
NATG	10	63	517	3.13	515	74	558	1.83

vertical motion, followed by an SH-like pulse with almost purely horizontal motion that is perpendicular to the horizontal movement in the initial pulse. The call at SNFQ (Fig. 5i,j) also has late SH-like motion, although it is much weaker than its initial pulse.

Note that the calls of Fig. 5c,d and Fig. 5e,f arrive only ∼2.5 s apart; they also appear as the doublet of calls at ∼63 s in Fig. 2f. Although we only show the waveforms from a single doublet of calls from this sequence, in each doublet the first call resembles that in Fig. 5c,d and the second call resembles that in Figure 5e,f. The completely different nature of their waveforms suggests that there are two whales singing from separate locations, rather than a single whale with an unusual song.

4 Discussion

The fin whale call in Figure 5e,f has >1 s of phase separation and is at LESQ, which is only 100 m from the shore. We interpret these as a P-like and S-like signals, although it is unclear to what degree they should be considered surface waves. This degree of phase separation suggests that the energy arriving at the receiver enters the solid earth near-source, rather than at the shoreline. Even if we assume $V_\mathrm{P} = 3$ km s^{-1} and $V_\mathrm{P}/V_\mathrm{S} = 2$ (representing a slow, porous, sedimentary layer) the implied source–receiver distance is $d = (1\text{ s})/(V_\mathrm{S}^{-1} - V_\mathrm{P}^{-1}) = 3$ km. We therefore suggest it is likely common that the energy arriving at onshore seismometers enters the earth almost entirely near-source (i.e. traveling most of the distance to

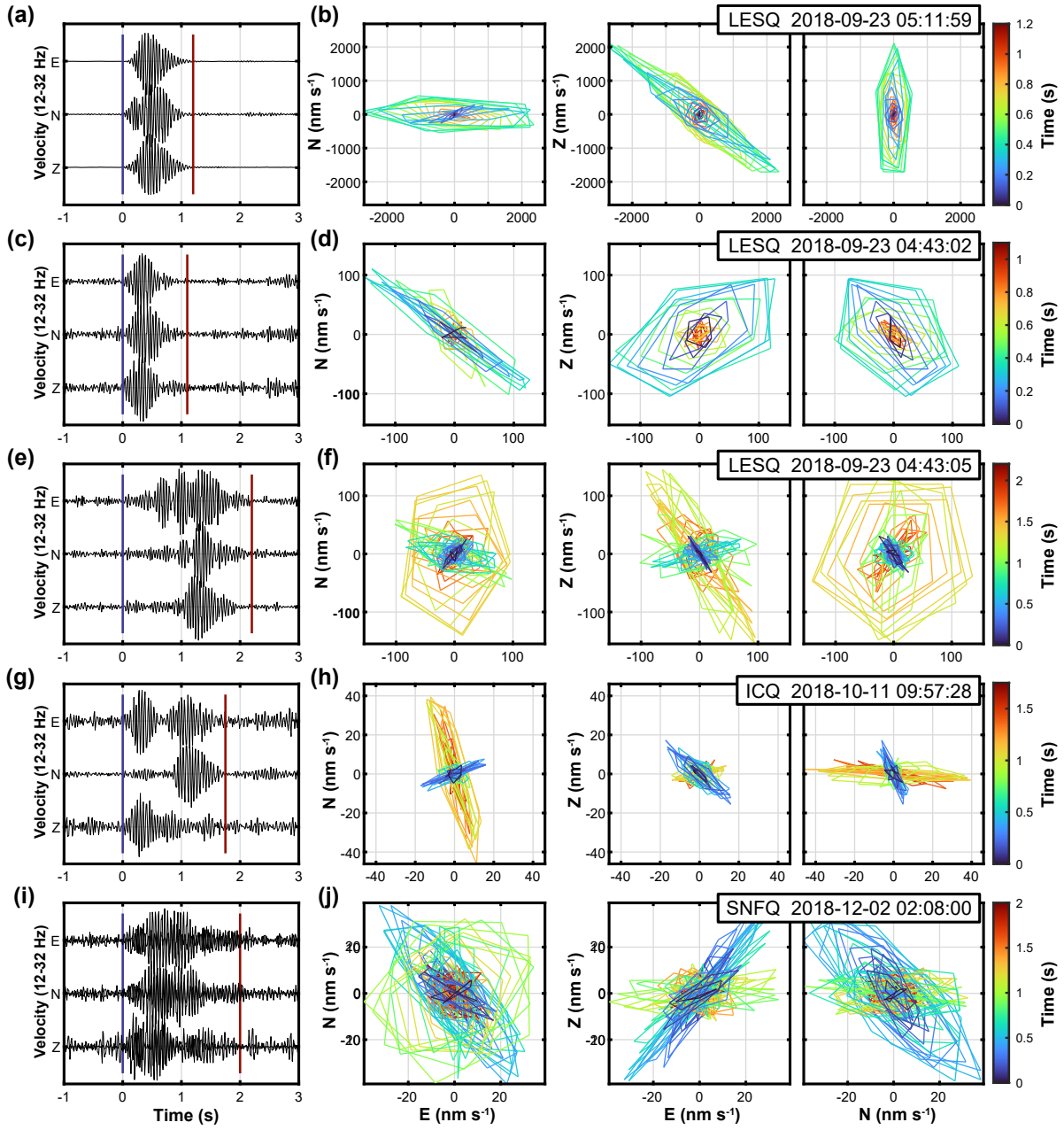

Figure 5. (a) Three-component waveforms of the maximum SNR fin whale call (the 4th fin whale call in Fig. 2e), from station LESQ. (b) Particle trace plots in the E–N, E–Z, and N–Z planes of the same fin whale call. (c,d)–(i,j) are equivalent figures for four other calls, at the labeled seismometers and UTC times. Note that (c,d) and (e,f) illustrate the first and second calls, respectively, of the two-whale sequence shown in Fig. 2f.

shore underground). There could be exceptions where the energy is mainly trapped in the water column until it reaches shore, or where both the solid- and water-paths contribute significantly (with energy from the solid-path arriving first), which is another plausible interpretation of the phase separation in Fig. 5e,f. Coupling within shallow sediment layers and at the sediment–bedrock interface are probably where much of energy is converted to S waves. For simplistic earth structure models, we would expect S energy to be constrained to the SV plane (the vertical plane containing the ray-path) as appears to be the case in Fig. 5a–d. However, the calls in Fig. 5e–j all last ∼2 s and appear to have significant SH motions (horizontal, perpendicular to the ray-path) as appears most prominently at $t > 1$ s in Fig. 5h,j. The presence of SH (potentially Love) waves implies substantial heterogeneity and complex travel paths within the solid earth. The low amount of shared detection times between neighboring seismometers suggests that their detection radius for whale calls is generally on the order of a few kilometers, although station SMQ has one of the larger catalogs for both fin and blue whale detections and is over 11 km from shore, indicating that some stations have a larger detection radius. Nevertheless, this is still considerably shorter than typical fin whale detection ranges on hydrophones, which are typically thought to be 30–40 km in shallow water (e.g. Širović et al., 2007; Cholewiak et al., 2018). Local noise conditions at each station are likely a major influence on their effective detection radii. Offshore geological and bathymetric factors may also impact the degree to which whale call energy is transferred from water into the earth. Full waveform modeling may illuminate what factors are critical for producing strong signals at onshore seismometers, although the earth models used would likely have to be 2D and incorporate the offshore to onshore transition. Ideally we would be able to compare our detection catalogs directly with a comparable catalog from hydrophones. However, hydrophones in the region are sparse, so while we can confirm that we see similar seasonal trends to Roy et al. (2018), a more detailed comparison is difficult.

Previous studies that have located whales with OBS, which are generally 4-component instruments with a hydrophone and three orthogonal geophones, have done so either with triangulation methods similar to those typically used for earthquake epicenters (e.g. Gaspà Rebull et al., 2006; Wilcock, 2012), or with single-station methods that rely on waveform polarization measurements to determine the azimuth of the incoming waves (e.g. Kuna and Nábělek, 2021). The vast majority of calls we record are only detected at a

single seismometer, and they generally have unclear phase and/or high noise levels that inhibit reliable azimuthal estimates, so neither method is easily applicable with the existing onshore data. There are certainly ways one could attempt to extract further information from these data, such as cross-correlating waveforms from neighboring stations to achieve relative delay times of whale signals, or perhaps cross-correlating waveform envelopes (e.g. Wech and Creager, 2008) is better suited to such high-frequency signals. However, a denser network of onshore seismometers and/or OBS in the LSLS is likely required to be able to triangulate sources, to clarify what seismic phases are arriving at seismometers, and to apply more advanced (e.g. cross-correlation–based) methods.

OBS are frequently equipped with hydrophones that have flat instrument response to much higher frequencies ($\gg$1000 Hz) than the geophone components (e.g. Nedimović, 2019), allowing them to record high-frequency calls from a broader range of cetacean species. Seafloor instruments have the obvious advantage of proximity to the whales and direct travel paths (without complications from interaction with earth structure), although having to avoid areas of trawl fishing may limit the potential deployment locations in the LSLS. Nodal seismometers are small instruments designed for rapid, short-term (onshore) deployments, that can usually record at sample rates of up to 1000 sps (e.g. Ringler et al., 2018). This is sufficiently high frequency to allow detection of NARW calls (50–350 Hz), in addition to fin and blue whale calls, so nodal seismometers present an excellent and inexpensive way to supplement data from offshore instruments. A hybrid deployment of ocean-bottom and nodal seismometers in the LSLS could potentially provide precise tracking of NARWs, fin, and blue whales. Such an experiment could be designed to jointly benefit earthquake science in the LSLS (Plourde and Nedimović, 2021), both by directly recording local earthquakes and using whale calls to probe shallow earth structure (Kuna and Nábělek, 2021).

5 Conclusion

We demonstrate that fin and blue whale calls can be observed at onshore seismometers and that these observations are common in the LSLS. Onshore seismometers appear to only detect calls from within a short radius, such that most calls are only detected at a single station. Fin whale calls often appear as a complex sequence of phases over $\sim$2 s. Therefore, although a network of OBS is likely necessary to produce

high-resolution tracks of whale locations, onshore seismometers could provide useful complimentary data. High–sample-rate nodal seismometers are inexpensive to purchase and use, and would allow for monitoring of NARW calls for short-term deployments. There are presumably many other regions with elevated risk of human-whale interaction, like the LSLS, that already have onshore seismometers in place for earthquake monitoring. These seismometers could potentially be an important component of real-time fin and blue whale monitoring networks.

Acknowledgments

The seismic waveform data used in this study is freely available from Earthquakes Canada (2021) at http://earthquakescanada.nrcan.gc.ca/stndon/AutoDRM/index-eng.php, (accessed July 2021). This work was supported by NSERC through a Discovery Grant to MRN.

Conflict of Interest Statement

The authors declare no competing interests.

Authors' Contributions

APP designed the methodology, led the application, and led writing of the manuscript. MRN conceived the premise of the study, and contributed critically to the methodology and writing.

References

Cholewiak, D., Clark, C.W., Ponirakis, D., Frankel, A., Hatch, L.T., Risch, D., Stanistreet, J.E., Thompson, M., Vu, E. and Van Parijs, S.M. (2018) Communicating amidst the noise: modeling the aggregate influence of ambient and vessel noise on baleen whale communication space in a national marine sanctuary. *Endangered Species Research, 36*, 59–75. https://doi.org/10.3354/esr00875

Dunn, R.A. and Hernandez, O. (2009) Tracking blue whales in the eastern tropical pacific with an

ocean-bottom seismometer and hydrophone array. *The Journal of the Acoustical Society of America, 126*, 1084–1094. https://doi.org/10.1121/1.3158929

Earthquakes Canada (2021) Canadian National Seismograph Network. *Geological Survey of Canada*. https://doi.org/10.7914/SN/CN

Gaspà Rebull, O., Cusí, J.D., Ruiz Fernández, M. and Muset, J.G. (2006) Tracking fin whale calls offshore the Galicia Margin, North East Atlantic Ocean. *The Journal of the Acoustical Society of America, 120*, 2077–2085. https://doi.org/10.1121/1.2336751

Harris, D.V., Miksis-Olds, J.L., Vernon, J.A. and Thomas, L. (2018) Fin whale density and distribution estimation using acoustic bearings derived from sparse arrays. *The Journal of the Acoustical Society of America, 143*, 2980–2993. https://doi.org/10.1121/1.5031111

Kirsebom, O.S., Frazao, F., Simard, Y., Roy, N., Matwin, S. and Giard, S. (2020) Performance of a deep neural network at detecting North Atlantic right whale upcalls. *The Journal of the Acoustical Society of America, 147*, 2636–2646. https://doi.org/10.1121/10.0001132

Kuna, V.M. and Nábělek, J.L. (2021) Seismic crustal imaging using fin whale songs. *Science, 371*, 731–735. https://doi.org/10.1126/science.abf3962

Mellinger, D.K. and Clark, C.W. (2003) Blue whale (Balaenoptera musculus) sounds from the North Atlantic. *The Journal of the Acoustical Society of America, 114*, 1108–1119. https://doi.org/10.1121/1.1593066

Mellinger, D.K., Stafford, K.M., Moore, S.E., Dziak, R.P. and Matsumato, H. (2007) An overview of fixed passive acoustic observation methods for cetaceans. *Oceanography, 20*, 36–45.

Mouy, X., Bahoura, M. and Simard, Y. (2009) Automatic recognition of fin and blue whale calls for real-time monitoring in the St. Lawrence. *The Journal of the Acoustical Society of America, 126*, 2918–2928. https://doi.org/10.1121/1.3257588

Nedimović, M.R. (2019) Ocean bottom seismometer instrumentation in Canada. *CSEG Recorder, 44*, 12–17.

Parks, S.E., Urazghildiiev, I. and Clark, C.W. (2009) Variability in ambient noise levels and call parameters of North Atlantic right whales in three habitat areas. *The Journal of the Acoustical Society of America, 125*, 1230–1239. https://doi.org/10.1121/1.3050282

Pettis, H., Pace, R.I. and Hamilton, P. (2021) North Atlantic Right Whale consortium 2020 annual report card. *Report to the North Atlantic Right Whale Consortium.*

Pilkington, J.F., Stredulinsky, E.H., Abernethy, R.M. and Ford, J.K. (2018) Patterns of fin whale (Balaenoptera physalus) seasonality and relative distribution in Canadian Pacific waters inferred from passive acoustic monitoring. *DFO Canadian Science Advisory Secretariat Research Document*, p. 032.

Plourde, A.P. and Nedimović, M.R. (2021) Earthquake depths, focal mechanisms, and stress in the Lower St. Lawrence Seismic Zone. *Seismological Research Letters, 92*, 2562–2572. https://doi.org/10.1785/0220200429

Ramp, C., Delarue, J., Bérubé, M., Hammond, P.S. and Sears, R. (2014) Fin whale survival and abundance in the Gulf of St. Lawrence, Canada. *Endangered Species Research, 23*, 125–132. https://doi.org/10.3354/esr00571

Ramp, C., Gaspard, D., Gavrilchuk, K., Unger, M., Schleimer, A., Delarue, J., Landry, S. and Sears, R. (2021) Up in the air: drone images reveal underestimation of entanglement rates in large rorqual whales. *Endangered Species Research, 44*, 33–44. https://doi.org/10.3354/esr01084

Ringler, A.T., Anthony, R.E., Karplus, M., Holland, A. and Wilson, D.C. (2018) Laboratory tests of three z-land fairfield nodal 5-hz, three-component sensors. *Seismological Research Letters, 89*, 1601–1608. https://doi.org/10.1785/0220170236

Rolland, R.M., Parks, S.E., Hunt, K.E., Castellote, M., Corkeron, P.J., Nowacek, D.P., Wasser, S.K. and Kraus, S.D. (2012) Evidence that ship noise increases stress in right whales. *Proceedings of the Royal Society B: Biological Sciences, 279*, 2363–2368. https://doi.org/10.1098/rspb.2011.2429

Roy, N., Simard, Y., Aulanier, F. and Giard, S. (2018) Fin whale continuous frequentation of St. Lawrence

habitats detected from multi-year passive acoustic monitoring (PAM). *DFO Canadian Science Advisory Secretariat Research Document*, p. 059.

Simard, Y., Roy, N., Giard, S. and Aulanier, F. (2019) North Atlantic right whale shift to the Gulf of St. Lawrence in 2015, revealed by long-term passive acoustics. *Endangered Species Research, 40*, 271–284. https://doi.org/10.3354/esr01005

Širović, A., Hildebrand, J.A. and Wiggins, S.M. (2007) Blue and fin whale call source levels and propagation range in the southern ocean. *The Journal of the Acoustical Society of America, 122*, 1208–1215. https://doi.org/10.1121/1.2749452

Širović, A., Rice, A., Chou, E., Hildebrand, J.A., Wiggins, S.M. and Roch, M.A. (2015) Seven years of blue and fin whale call abundance in the southern california bight. *Endangered Species Research, 28*, 61–76. https://doi.org/10.3354/esr00676

Watkins, W.A., Tyack, P., Moore, K.E. and Bird, J.E. (1987) The 20-Hz signals of finback whales (Balaenoptera physalus). *The Journal of the Acoustical Society of America, 82*, 1901–1912. https://doi.org/10.1121/1.395685

Wech, A.G. and Creager, K.C. (2008) Automated detection and location of Cascadia tremor. *Geophysical Research Letters, 35*, L20302. https://doi.org/10.1029/2008GL035458

Wilcock, W.S.D. (2012) Tracking fin whales in the northeast Pacific Ocean with a seafloor seismic network. *The Journal of the Acoustical Society of America, 132*, 2408–2419. https://doi.org/10.1121/1.4747017